PEROVSKITE CATALYSTS FOR THE CATALYTIC FLAMELESS COMBUSTION OF METHANE. PREPARATION BY FLAME-HYDROLYSIS AND CHARACTERISATION BY TPD-TPR-MS AND EPR

R. Leanza, I. Rossetti, L. Fabbrini, C.Oliva and L. Forni[*]

Dipartimento di Chimica Fisica ed Elettrochimica e Centro CSRSRC.CNR,

Università di Milano, via Golgi, 19   I-20133 Milano, Italy

ABSTRACT

A new method was employed for the preparation of a set of lanthanum cobaltites of general formula $La_{1-x}M_xCoO_{3+\delta}$ with M=Ce, Eu and x=0, 0.05, 0.1, 0.2. All the samples so prepared showed nanostructured, thermally very stable and characterised by highly crystalline perovskite-like structure and high surface area. Their activity as catalysts for the catalytic flameless combustion of methane was by *ca.* one order of magnitude higher than that of their analogues, prepared through the usual calcination-milling procedure. Adsorption of oxygen was accompanied by formation of paramagnetic species. Desorption of preadsorbed oxygen was dependent on the nature of the doping element and on the value of the stoichiometric coefficient *x* of their formula. A correlation between the temperature of the maximal rate of oxygen release and catalytic activity was found. The following scale of activity for the title reaction *vs. x* values could be set up: 0.1 Ce > 0.05 Ce > 0 > 0.05 Eu > 0.1 Eu $\cong$ 0.2 Ce. The higher activity of Ce-doped catalysts as compared to those doped with Eu was found to be related to the strength of the bond between oxygen and Co ions.

Keywords: Perovskite-like catalysts; Flame-hydrolysis preparation method; Methane catalytic combustion; TPD-TPR-MS characterisation; EPR, particle size effect

---

[*] Corresponding author. Phone: +39-02-26603289, Fax: +39-02-70638129, E-mail: l.forni@csrsrc.mi.cnr.it

INTRODUCTION

Catalytic (flameless) combustion (CFC) of hydrocarbons has gained attention in the recent past in order to limit environment pollution. Indeed, the temperature attained in catalytic burners (below 800°C) is much lower than in usual burners, so limiting or virtually suppressing any NO_x formation. The so far mostly employed catalysts for CFC are supported noble metals, which, however, besides being expensive, can generate harmful compounds and may sinter rather easily. Mixed oxides of perovskitic structure showed a valuable alternative to such catalysts, being much cheaper, thermally stable and comparatively active. Their general formula is ABO_3, where A is usually a rare earth cation and B a transition metal cation. Both A and B cations can be substituted to some extent, leading to a large class of materials of general formula $A_{1-x}A'_xB_{1-y}B'_yO_{3\pm\delta}$, possessing different properties. In the formula δ represents the excess of oxygen due to non-stoichiometry of these species. Particularly, the nature and the amount of the substituent at A position can stabilise unusual oxidation states for the B cation and/or generate anionic vacancies in the solid [1]. These structural defects bring about the modification of some physico-chemical properties, so favouring *e.g.* ions transport within the oxide framework. This entrains interesting differences in catalytic behaviour.

Voorhoeve and co-workers [2] discussed such properties and proposed a "suprafacial" and an "intrafacial" reaction mechanism for hydrocarbons oxidation over these catalysts. The former mechanism rises from the interaction of surface oxygen with reactants and it is operative at low temperature (T<400°C). The latter is effective at higher temperature (T>400°C) and involves a redox cycle, in which bulk oxygen migrates toward the surface, becoming available for the oxidation of the substrate, and it is replaced by gaseous oxygen, through a Mars-Van Krevelen mechanism. The mobility of O^{2-} ions in the crystalline framework determines the mechanism of the actual catalytic reaction. Both

mechanisms are usually observed with perovskites, which are characterised by many different structural defects. Temperature Programmed Desorption- and Temperature Programmed Reaction-Mass Spectrometry (TPD-TPR-MS) can be valuable tools to determine catalyst affinity for oxygen and the dependence of activity on temperature. During TPD analysis of pre-adsorbed oxygen two desorption peaks are usually observed, called α and β, corresponding to surface- and bulk-oxygen release, respectively [3].

From a practical point of view, the preparation procedure is of fundamental importance to determine both activity and durabilty of the catalyst. Various preparation methods can be found in literature [4-10], but high surface area and thermal resistance to sintering are not easy to be obtained simultaneously by those procedures. Indeed, in order to enhance catalyst activity, a high surface area (20-30 m^2/g) is needed. However, this is usually obtained by calcining the catalyst at relatively low temperature (700-750°C), which leads to insufficient thermal stability of the solid. A solution of the problem can be the synthesis of highly dispersed 'nanostructured' powder materials, obtainable by the flame hydrolysis (FH) technique, which was successfully applied to other materials [11,12].

In the present work a set of Lanthanum cobaltites of general formula $La_{1-x}M_xCoO_{3\pm\delta}$, with M = Eu, Ce and x = 0, 0.05, 0.1, 0.2 was prepared by a new FH procedure [13]. The samples were characterised and tested as catalysts for the CFC of methane, aiming at comparing their physico-chemical properties and activity with those of samples of the same composition, but prepared by other methods.

EXPERIMENTAL

Catalysts Preparation

A detailed description of the apparatus and of the conditions adopted for perovskites preparation can be found elsewhere [13]. Briefly, a *ca.* 3 wt.% solution in 10% HNO_3 of the precursor salts ($La(CH_3COO)_3$, $Co(CH_3COO)_2$, $Eu(CH_3COO)_2$ and $Ce(NO_3)_3$, by ALDRICH and MERCK) was prepared, to which citric acid was added, in 0.5/1 molar ratio with respect to the sum of metal salts. HNO_3 and citric acid were added in order to help the dissolution of the metal salts and to form a complex hindering the precipitation of some solid compound, respectively. The solution was nebulised by means of a home-made nozzle into a H_2+O_2 flame. The estimated temperature of oxides formation was 1600-1800 °C. The residence time of reagents in the flame hottest zone was estimated to be less than 0.1 s. The finely powdered solid so produced was collected by means of a 10 kV electrostatic precipitator. Two comparative samples were also prepared by the usual repeated high-temperature (950-1050°C) calcination-milling (CM) and sol-gel citrate (SGC) methods, respectively. The main characteristics of the catalysts so prepared are collected in Table 1.

Catalysts characterisation

X-ray diffraction analysis (XRD) was done by means of a Philips PW 2273/20 diffractometer, using the Ni-filtered Cu Kα radiation (λ=1.5418 Å). Phase recognition was obtained by comparison with literature data [14]. BET surface area and porosity were determined by nitrogen adsorption/desorption by means of a Micromeritics ASAP 2010 instrument. A Cambridge Stereoscan 150 Scanning Electron Microscope (SEM) was employed for morphological analysis and for determining the particle size. The composition of the catalysts was checked through XRF analysis by means of a Jordan-Valley (mod. EX 310) instrument. The calibration of the latter has been made by the analysis of oxide mixtures of known composition.

TPD-TPR analysis

A detailed description of the TPD-TPR-MS apparatus was given elsewhere [15]. 0.8 g of catalyst, pressed into wafers, then ground and sieved to 0.15-0.25 mm particles, were loaded in a quartz reactor heated by an electric furnace through an Eurotherm (mod. 822) TRC, controlled by a thin thermocouple located within the catalyst bed. Helium (purity$\geq$99.9999 vol. %) was employed as carrier gas. Air (purity$\geq$99.9995 vol. %) was used for oxygen pre-saturation of catalyst in TPD-MS analysis, while methane (1.04% in helium) was employed in addition to air in TPR-MS experiments. The outlet gas was analysed by means of a quadrupolar mass spectrometer (QMS) (mod. PPT Residual Gas Analyser, by MKS Instruments).

The catalyst was activated by running a temperature ramp of 10°C/min from 50°C to 800°C, while flushing with helium (20 cm^3/min). The final temperature was maintained till the signals relative to H_2O (m/z=18), CO_2 (m/z=44), O_2 (m/z=32), NO (m/z=30) and CO (m/z=28) became stable. A further pre-treatment in 40 cm^3/min flowing air at 750°C was done overnight in order to clean the sample by burning off any possible residua from citrates. After lowering temperature to 50°C in flowing air, the carrier gas was switched to helium (20 cm^3/min) and the system kept at 50°C till the stability of signals. A 10°C/min temperature ramp was then started from 50°C up to the final isotherm at 800°C, kept for 10 minutes.

In TPR-MS analysis the same pre-treatment and temperature programme was followed, with helium (20 cm^3/min) as carrier gas. The runs were carried out by injecting 1.2 cm^3 pulses of the reacting gas mixture. This was composed of 0.5 vol. % methane, 50 vol. % air and 49.5 vol. % He. The species monitored were CH_4 (m/z=15, in order to avoid

confusion with the m/z=16 fragment of O_2), H_2O (m/z=18), N_2 (m/z=14, to distinguish it from CO), O_2 (m/z=32), CO_2 (m/z=44), CO (m/z=28) and NO (m/z=30).

EPR analysis

EPR spectra have been collected by means of a Bruker mod. ESP 300 spectrometer operating at *ca.* 9.4 GHz. Their simulation was done by the SimFonia (Bruker) software. The high-frequency (240 GHz) spectra were recorded by means of a special apparatus home-assembled at IFAM CNR (Pisa).

Catalytic activity tests

The activity in methane combustion was tested by means of a bench-scale continuous apparatus. 0.2 g of catalyst, pressed into wafers, ground and sieved to 0.15-0.25 mm particles, were loaded in a vertical, downflow quartz reactor (7 mm ID, fitted with a 1.6 mm OD axial thermowell) after dilution with 1.3 g of quartz powder of the same particle size. The catalyst bed was kept in the isothermal middle part of the reactor by quartz wool. The void part of the reactor tube, above and below the catalyst bed, was filled with quartz beads (0.25-0.85 mm). CH_4 (1.04 vol. % in He) and air flow rates were regulated by means of mass flow-meters (MKS Instr., mod. 1259 CC) and MKS mod. 247C control unit. The reactor was heated in an electric furnace using an EUROTHERM mod. 812 TRC. The outlet gas was analysed by means of a HWD gas-chromatograph (HP mod. 5890 A), equipped with Porapak Q and MS 5A columns. Prior to each run the catalyst was activated by flowing 20 cm^3/min of air while increasing temperature by 10°C/min up to 600°C, then kept for 1 h. The activity tests were carried out by feeding 20 cm^3/min of a gas mixture composed of 10 cm^3/min of 1.04% CH_4 in He and 10 cm^3/min of air, while increasing the temperature by 2 °C/min from 250 up to 600°C.

RESULTS AND DISCUSSION

Crystallinity, surface area and particle size

All the present catalysts were characterised by high crystallinity, as shown by the sharp XRD reflections (Fig.1). The perovskite phase was recognised by the typical signals at $2\theta=23, 40, 46, 54, 59$ degrees [14]. Moreover, high phase purity was achieved for every sample except for sample no.*4* (Table 1), in which segregation of CeO_2 was noticed (Fig.1). Furthermore, for each sample SEM analysis showed agglomerates, 200-500 nm in size, made of highly uniform, nearly spherical particles, 20 to 80 nm in size (Fig. 2), by *ca.* one order of magnitude smaller than those shown by the SGC sample (Table 1).

BET surface area was always around 20 m^2/g (Table 1), confirming the efficacy of the preparation method. Indeed, the very short calcination time, characteristic of the FH technique, limits any significant sintering of the powder. Surface area of FH samples was *ca.* five times higher than that of the comparison sample prepared by the CM method while it was nearly of the same magnitude of that of the comparison sample prepared by the SGC procedure [16].

Furthermore, FH samples proved to be thermally very stable at the methane CFC temperature, being prepared at a temperature nearly 1000°C higher. However, no correlation was found between surface area and both the nature and the concentration of either of the dopants. The X-ray fluorescence (XRF) analysis showed that the composition of all the samples was very close (within an error of $\pm1\%$) to the nominal one.

TPD-MS analysis

The above mentioned α and β peaks (see Introduction) originate from the different oxidation states of cobalt and from the presence of structural defects in the crystal lattice

of the perovskite [16-18]. β oxygen is usually released at a temperature higher than 700°C, when bulk oxygen migrates very quickly. The results are shown in Fig. 3.

Substitution of either Ce^{4+} or Eu^{2+} for La^{3+} showed to affect both types of oxygen desorption. However, the β peak started to grow at ca. 700°C for all our samples, suggesting that this peak is connected with the oxidation state of the Co ion. Indeed, the temperature of its onset is close to that (895°C) of thermal decomposition of Co_2O_3. Neither CoO, nor CeO_2 decompose on heating in air. They simply melt at 1795 and *ca.* 2600°C, respectively. As a consequence, some researchers attributed the release of β oxygen to Co^{3+}/Co^{2+} reduction [17]. By contrast, the α peak appears to be strongly dependent on the nature of the dopant substituting for La and on the substitution degree. This peak has been attributed to Co^{4+} reduction to Co^{3+}, where Co^{4+} was formed by the substitution of M^{n+} (n<3) for La^{3+}. Therefore, α peak is correlated to the concentration of surface anionic vacancies. The latter, however, cannot explain the particular dependence of α peak area on the degree of lanthanum substitution, observed with our samples (Fig. 3). Indeed, the partial Eu^{2+} substitution for La^{3+} would increase the concentration of anionic vacancies, so leading to a simultaneous increase of the α peak area, while the substitution with Ce^{4+} should bring about the opposite effect. However, these effects can be observed for the *x* = 0.05 substitution degree only (Fig. 3, samples *1*, *2* and *5*). Indeed, the α peak area relative to catalyst no.*2* is lower and that of catalyst no.*5* is higher than the α peak area of catalyst no.*1*. By contrast, for *x* = 0.1 (Fig. 3, samples *3*, and *6*) both the dopants seem to have a similar effect, because the α peak areas are larger than that of catalyst no.*1*. With a further increase of Ce substituting for La (catalyst no.*4*) the α peak area becomes even larger than for catalyst no.*3*. This can be attributed to the partial segregation of Ce as CeO_2 (see Fig. 1), leading to a less ordered structure. The same phenomenon was noticed by others through XRD analysis [18] showing CeO_2 as

secondary solid phase, so that cationic vacancies formed, due to non-complete insertion of the dopant into the perovskite framework.

Another interesting feature of the α-peak signal of our samples is the shift of the temperature T_{MAX}, corresponding to the desorption peak maximum, with changing the dopant nature and the substitution degree (Fig. 4). The trend parallels that of the concentration of anionic vacancies in the solid, which decreases with increasing the degree of Ce-doping and grows with increasing the Eu-doping. Notice, however, that the value of T_{MAX} for catalyst *2* is rather uncertain, due to the very low intensity of the signal, largely masked by the noise (Fig. 3, sample *2*).

In the present case, the Eu-doped samples *5* and *6*, richer in anionic vacancies, showed values of T_{MAX} higher than 400°C. By contrast, Ce addition (samples *3* and *4*) led to T_{MAX} lower than 400°C, because of a decrease of concentration of anionic vacancies. The higher the concentration of surface anionic vacancies, the lower should be the tendency of oxygen to leave the catalyst surface for oxidizing the substrate. Therefore, on the base of this analysis, samples *3* and *4* are expected to be the best catalysts. Indeed, an easy release of oxygen from the catalyst surface is a fundamental property in determining the activity for the low-temperature oxidation of methane. However, this is not sufficient, as shown by the relatively high values of light-off temperature of Ce-doped samples [16].

TPR-MS analysis

The typical trend of the m/z=15 signal, relative to injected methane pulses, is reported in Fig. 5. A similar trend was shown for the consumption of oxygen and a corresponding progressive increase was noticed for the formation of carbon dioxide. Carbon and nitrogen monoxides were never detected in any of our experiments, as

expected, due to the low temperature of reaction. This confirms the high selectivity of all the present samples for the complete oxidation of the reactant and the absence of NO_x formation in methane catalytic combustion over perovskites. By these TPR-MS experiments, it has been possible to calculate T_b, $T_{1/2}$ and T_{cc}, representing the temperature of light-off, of 50% and of 100% conversion of methane, respectively. The values are collected in Table 2.

A correlation between T_{MAX} and $T_{1/2}$, determined by the TPR-MS analysis, points out that the most active catalyst was sample *3*, showing the lowest value of T_{MAX}, *i.e.* the lowest temperature for oxygen desorption.

These results allow to set up the following scale of activity for our samples: *3 > 2 > 5 > 6 $\cong$ 4*. This confirms the beneficial effect of low-concentration ($x \le 0.1$) Ce-doping and the opposite unbeneficial effect of Eu-doping on the activity of La cobaltites. The exception of catalyst *4*, which showed an activity much lower than expected, is due to the too high substitution degree, bringing about a partial segregation of CeO_2, as previously mentioned.

EPR analysis

The freshly prepared $LaCoO_3$ sample (no. *1,* Table 1) was characterised by an EPR pattern composed of more contributions (Fig.6*a*). Some days later the spectral shape changed, as shown in Fig.6*b* for the EPR spectrum recorded at 165 K with a ten-days aged sample. The difference between these two patterns (Fig.6*c*) shows that during the ageing of the sample the contribution at $g \cong 2.35$ disappeared, while the signal at $g \cong 2$ decreased with respect to the main broad symmetric feature. The latter can be fitted by a single Lorentzian-shaped line with $g \cong 2.16$ and with peak-to-peak width ΔH_{pp} of *ca*. 500 G, nearly independent of temperature. A line of this kind has been observed also with

oxygen-deficient Co_3O_4 [20], as well as with SGC-prepared $La_{0.9}Ce_{0.1}CoO_{3\pm\delta}$ [21] and attributed to superexchange between $3d^7$ Co^{2+} ions ($S = 1/2$) mediated by O^{2-} in $-Co^{2+}-O^{2-}-Co^{2+}-O^{2-}-$ chains. In the latter example, these chains were formed after use for catalytic reduction of NO by CO. Indeed, it was hypothesised that, during that reaction, surface oxygen vacancies were filled by oxygen atoms coming from NO molecules. In both the above cited situations the EPR line was broader than in the present case, and further linearly broadening with increasing temperature, due to a phonon-dependent electron spin relaxation process. This different behaviour could be explained on the basis of the smaller size of the particles obtained by the FH procedure, combined with the high electrical conductivity of these systems. This property is revealed by the $g \cong 2$ line of Fig. 6, attributable [26,27] to "nearly free" conduction electron, and confirmed by the fact that the present SEM analysis could be made even without sample gilding. Indeed, it has been reported [23] that the spin-spin relaxation is slower in smaller "metametallic" metal carbonyl clusters than in bulk samples and that 25 nm particles of $La_{1-x}Ca_xMnO_3$ ($x=0.3$) give EPR spectra with smaller line-width values than 3500 nm particles of the same composition [24]. The size-dependent relaxation process leads to slower electronic relaxation rates for nano-structured paramagnetic particles and, therefore, to narrower EPR lines [25]. In the present investigation the SEM analysis shows that FH-prepared catalyst particles are nearly one tenth smaller than for the sample prepared by the SGC method. Therefore, narrower EPR lines are indeed to be expected with FH samples. In addition, FH-prepared particles are too small for ordered chains, suitable to phonon propagation, to form. Instead, only local dipolar and exchange interactions should arise in small Co-O clusters.

When 10% Ce or Eu substituted for La, the shape of the main broad EPR spectrum changed and its intensity reduced by nearly 80% (Fig.7, *a* and *b*, respectively).

After a few days the spectum obtained with the Eu-doped catalyst became similar to that reported in Fig.7a for the Ce-doped sample. This line should be due to oxygen interacting with cobalt ions. Indeed, oxygen-only paramagnetic species are characterised [26] by EPR lines with g values lower than 2.046. After a few months ageing, the EPR spectra obtained with the two dopants did not differ significantly with each other and the contribution at $g \cong 2.13$ was no more detectable, due to the decreased spectral intensity.

The formation of (S = 3/2) $3d^7 Co^{2+}$ ions tetrahedrally coordinated to four oxygen atoms could be the situation indicated by the $g \cong 2.35$ line observed (Fig.6) with the present freshly prepared LaCoO$_{3\pm\delta}$ sample. However, these ions are characterised by very fast relaxation times and, therefore, they are observable only at very low temperature. Therefore this EPR line is more likely due to the formation of some $Co^{3+}(S=0)/O_2^{-}(S=1/2)$ pairs. The presence of these ion-pairs has been hypothesised elsewhere [6] as a consequence of the O_2 adsorption on Co^{2+}. However, the present $g \cong 2.35$ EPR line disappeared within a few days (Fig.6b), suggesting that this species is rather unstable in the undoped LaCoO$_{3\pm\delta}$ sample.

By contrast, paramagnetic species characterised by a $g \cong 2.3$ EPR line are by far more stable with Ce- and Eu-containing catalysts. Indeed, their presence is revealed by the EPR patterns detected with these samples immediately after their preparation (Fig.7), as well as with the same samples after a nine months ageing. These aged samples have been also examined by High-Frequency (240 GHz) EPR Spectroscopy (Fig. 8). By this technique, the $g \cong 2.3$ spectral region further resolved into two lines at g = 2.336; 2.308, and at g = 2.29; 2.25, with the Ce- and with the Eu-containing samples, respectively. The only difference between the EPR spectra obtained with the two dopants was that the g values were a bit higher with Ce than with Eu, indicating that oxygen binds to Co ions more tightly in the former than in the latter case.

The above mentioned results differ rather markedly from those reported elsewhere by us with $La_{0.9}M_{0.1}CoO_{3\pm\delta}$ (M = Eu, Ce) samples (there labelled as HN), prepared by the SGC procedure [19]. Indeed, at room temperature the EPR spectrum of the undoped HN sample was composed of a broad asymmetric pattern at $g \cong 2$, to which a second feature added at the external magnetic field value of *ca.* 1000 G. At lower temperature, this line broadened and moved towards lower field values. With the HN Eu-doped sample this low-field line was observed at $T < 235$ K only. A similar behaviour was observed also with the Ce-doped sample, but this low-field line was by far less intense.

This line was there attributed to O^{-}_{ads} ions grouped onto the internal pores surface and forming *spin bags*, *i.e.* ferromagnetic domains in which the ferromagnetic attraction among O^{-}_{ads} overcomes the electrostatic repulsion among them. The presence of spin bags indicates that the sample oxidation process does not occur completely, *i.e.* that the catalyst activation process was incomplete. Therefore, the presence of spin bags in freshly prepared HN, but not in the present FH-prepared samples, indicates that more oxygen must be available on the external surface of the latter when employed as catalyst for oxidation reactions.

Catalytic activity tests

As already mentioned, perovskites can be employed for the CFC of hydrocarbons at temperature much lower than that reached in the usual combustion process. We have chosen the combustion of methane as model reaction because methane is very widely employed as fuel and it is the less reactive hydrocarbon.

All the present catalysts were highly active, leading to complete methane conversion to carbon dioxide at 550-600°C, under the selected reaction conditions (Fig. 9*a*). Furthermore (Fig. 9*b*), they behaved much better than catalysts *7* and *8,* prepared

with the CM and SGC methods, respectively. By comparing catalysts *1* to *6* (Fig. 9*a*), a scale of catalytic activity can be determined, depending on the nature of the dopant and of the degree of substitution. The temperatures of light off, of half-transformation and of complete conversion (T_b, $T_{1/2}$, T_{cc}, respectively, Table 2) were adopted as criteria for this comparison. These temperatures are shifted towards higher values with respect to those determined by the TPR-MS technique (same Table 2), largely due to the time-lapse between pulse injection and signal detection by the QMS. Furthermore, the determination of T_b was often difficult, due to the presence of low-temperature partial conversion through the suprafacial mechanism. Therefore, the values of this parameter reported in Table 2 are difficult to compare with those derived from the TPR-MS analysis. Hence, when possible, two values of the light off temperature are reported: $T_b{}^*$, referred to the onset of the suprafacial mechanism contribution, and T_b, indicating that of the intrafacial one.

Catalyst *3*, in which 10% Ce substituted for La, showed again the most active, leading to 50% conversion at 438°C and to complete conversion at 560°C. This confirms the above reported TPR-MS results. The less active catalyst was again no. *4*, in which 20% Ce substituted for La. $T_{1/2}$ was ca. 468°C and T_{cc} about 600°C for this sample. A suprafacial mechanism contribution was observed with samples *1*, *2*, *3* and *5*, leading to some conversion between 250 and 300°C. In spite of this, the same scale of activity was obtained, *i.e. 3 > 2 > 1 > 5 > 6 ≅ 4* (*vide supra*), further confirming all the previous results.

Furthermore, the trend of catalytic activity *vs*. La substitution degree was similar to that obtained with cobaltites synthesised by other methods [16]. Indeed, the electric charge disequilibrium brought about by the partial substitution of Ce^{4+} for La^{3+} is compensated by the formation of Co^{2+} species and/or by a decrease of the anionic vacancies concentration. The decrease of structural defects can favour the (low temperature) suprafacial mechanism, so explaining the higher activity of catalyst *3*.

However, a low T_{cc} value could hardly be explained on this basis only. More likely, the formation of Co^{2+} creates a variety of active sites, which make easier the regeneration of the catalyst through the redox cycle. Hence, gaseous oxygen can be reduced by Co^{2+} oxidation to Co^{3+} [16], with formation of paramagnetic pairs like *e.g.* Co^{3+}/O^{2-}, as revealed by the above mentioned EPR lines at $g \cong 2.3$ and at $g \cong 2.13$.

A further increase of cerium substitution for lanthanum (sample *4*), however, does not lead to higher activity. This can be due to the partial segregation of CeO_2, as mentioned, accompanying a degree of Ce substitution for La beyond 10%. An alternative explanation, according to other studies [17], is that a high substitution degree causes a great oxygen release and this would make more difficult the subsequent reoxidation of the surface, leading to lower activity.

Europium addition, instead, favours the Co^{3+} oxidation to Co^{4+}, which cannot be easily stabilised in the perovskite matrix. Its subsequent reduction is then favoured, accompanied by the release of oxygen from the framework and by the change, within a few days, of its EPR patterns. These are characterised by fast formation of the species revealed by the line at $g \cong 2.3$, and by the slow formation of those revealed by the line at $g \cong 1.35$, as above discussed. The result is the increase of the anionic vacancies, leading to an improvement of the low-temperature suprafacial mechanism above proposed on the base of the TPD-MS results.

CONCLUSIONS

The lanthanum cobaltites prepared by the flame-hydrolysis method proved to be highly crystalline, nanostructured, thermally stable materials of high surface area and, hence, of high activity. The most active catalyst was $La_{0.9}Ce_{0.1}CoO_{3\pm\delta}$, leading to complete conversion of methane at a temperature as low as 560°C.

Furthermore, at the same composition, FH-prepared samples are formed by spheroids by *ca.* one order of magnitude smaller than the SGC-prepared ones (HN), though possessing the same surface area. EPR analysis revealed that more internal pores are present in the latter, on the surface of which O^-_{ads} spin bags form, leading to a loss of oxygen availability when the sample is used as catalyst for an oxidation reaction.

At last, paramagnetic species involving both oxygen and cobalt ions (such as Co^{3+}/O_2^- pairs) form also with the undoped $LaCoO_{3+\delta}$ sample prepared by FH. However, these species disappear within a few days, while they are stabilised when 10% Ce or Eu substitutes for La, being then detectable even in nine months aged samples. In these samples the oxygen ion is a bit more tightly bound to cobalt with Ce- than with Eu-containing samples, as revealed by a *g* value of the corresponding EPR line, which was a bit higher for the former than for the latter catalysts. This explains the higher activity and stability of the Ce-doped FH-prepared samples for the chosen standard oxidation reaction.

ACKNOWLEDGEMENTS

REFERENCES

[1] - J. L. G. Fierro, in *Properties and Applications of Perovskite-Type Oxides*, Ed. L. G. Tejuca, J. L. G. Fierro, Dekker New York, 1993, pag. 195.

[2] - R.J.H. Voorhoeve, J.P. Remeika and D.W. Johnson, *Science*, 180 (1973) 62.

[3] - T. Seiyama, in *Properties and Applications of Perovskite-Type Oxides*, Ed. L. G. Tejuca, J. L. G. Fierro, Dekker New York, 1993, pag. 215.

[4] - M. S. G. Baython and F. R. Sale, J. Mater. Science, 17 (1982) 2757.

[5] - H. M. Zhang, Y. Teraoka, N. Yamazoe, Chem. Lett. (1987), 665.

[6] - L. Forni, C. Oliva, F. P. Vatti, M. A. Kandala, A. M. Ezerets, A. V. Vishniakov, Appl. Catal. B: Environmental, 7, (1996) 269.

[7] - D. W. Johnson Jr., P. K. Gallagher, F. J. Schnettler and E. M. Vogel, Ceram. Bull., 9, (1977), 785.

[8] - H. Fujii, N. Mizuno and M. Misono, Chem. Lett. (1987), 2147.

[9] - N. Mizuno, M. Misono and H. Fujii, Chem. Lett. (1986), 1333.

[10] - A. Gonzales, E. Martinez Tamayo, A. Beltran Porter, V. Cortes Corberan, Catal. Today, 33, (1997), 361.

[11] - J. Long et S. J. Teichner, Rev. Hautes Temper. et Refract., 2, (1965), 47.

[12] - W. R. Moser, Chim. Ind. (Milan), 80, (1998), 191.

[13] - R. A. M. Giacomuzzi, M. Portinari, I. Rossetti and L. Forni, Proc. 12th Intern. Congr. on Catalysis, Granada, July 2000, in press.

[14] - Selected Powder Diffraction Data, Miner. DBM (1-40), J.C.P.D.S., Swarthmore, PA, 1974-1992.

[15] - L.Forni, M. Toscano and P. Pollesel, *J. Catal.*, 130 (1991) 392.

[16] - D. Ferri and L. Forni, *Appl. Catal. B: Environmental*, 16 (1998) 119.

[17] - Y. Teraoka, M. Yoshimatsu, N. Yamazoe and T. Seiyama, *Chem. Lett.*, (1984) 893.

[18] - T. Nitadori and M. Misono, *J. Catal.*, 93 (1985) 459.

[19] - C.Oliva and L.Forni, *J.Appl. Magn. Reson.*, submitted.

[20] - C.Oliva, L.Forni and L.Formaro, *Applied Spectroscopy,* 1996, 50, 1395.

[21] - L.Forni, C.Oliva, T.Barzetti, E.Selli, A.M.Ezerets, A.V.Vishniakov, *Applied Catalysis B: Environmental*, 1997, 13, 35.

[22] - A.Abragam and B.Bleaney "Electron Paramagnetic Resonance of Transition Ions", Dover Publ., New York 1986, p.528 and p.470.

[23] - R.Benfield, J.Organom.Chem., 1989, 372, 163.

[24] - A.K.Srivastava, C.M.Srivastava, R.Mahesh and C.N.R. Rao, Solid State Commun., 1996, 99, 161.

[25] - R.Benfield, J.Phys.Chem., 1987, 91, 2712.

[26] - C.Oliva, G.Termignone, F.P.Vatti, L.Forni, A.V.Vishniakov, *J.Materials Sci.*, 1996, 31, 6333.

[27] - C.Oliva, L.Forni, A.M.Ezerets, I.E.Mukovozov and A.V.Vishniakov, *J.C.S.Faraday Trans.*, 1998, 94, 587.

TABLE 1: Main properties of the catalysts employed.

Cat.no.	Composition	S_{BET} (m^2/g)	Part. size (nm)
1	$LaCoO_3$	17.9	20-80
2	$La_{0.95}Ce_{0.05}CoO_{3\pm\delta}$	19.4	20-80
3	$La_{0.9}Ce_{0.1}CoO_{3\pm\delta}$	24.0	20-80
4	$La_{0.8}Ce_{0.2}CoO_{3\pm\delta}$	20.6	20-80
5	$La_{0.95}Eu_{0.05}CoO_{3\pm\delta}$	20.6	20-80
6	$La_{0.9}Eu_{0.1}CoO_{3\pm\delta}$	18.3	20-80
7	$La_{0.9}Ce_{0.1}CoO_{3\pm\delta}$ *	4.6	≥ 1000
8	$La_{0.9}Ce_{0.1}CoO_{3\pm\delta}$ **	22.0	400-600

* Prepared by the CM method

** Prepared by the SGC method

TABLE 2: Comparison between T_b, $T_{1/2}$ and T_{cc} determined through TPR-MS analysis and catalytic activity tests.

Cat. No.	TPR-MS analysis			Catalytic activity tests			
	T_b (°C)	$T_{1/2}$ (°C)	T_{cc} (°C)	T_b* (°C)	T_b (°C)	$T_{1/2}$ (°C)	T_{cc} (°C)
1	375	503	630	>290	380	466	>600
2	378	500	623	270	360	459	580
3	322	445	568	<250	340	438	560
4	370	530	691	/	345	468	600
5	372	512	653	250	360	450	580
6	434	525	619	/	360	462	580

(*) Referred to suprafacial mechanism contribution.

FIGURE CAPTIONS

Fig. 1: XRD patterns of Table 1 samples. (∇) indicates CeO_2 phase.

Fig. 2: Typical SEM picture of our FH-made catalysts (sample 3, Table 1).

Fig. 3: TPD-MS spectra of preadsorbed oxygen. Numbers refer to the catalyst no. (Table 1).

Fig. 4: Dependence of T_{MAX} on the nature of the dopant and the substitution degree. Datum for catalyst 2 is rather uncertain, due to the very low intensity of the signal.
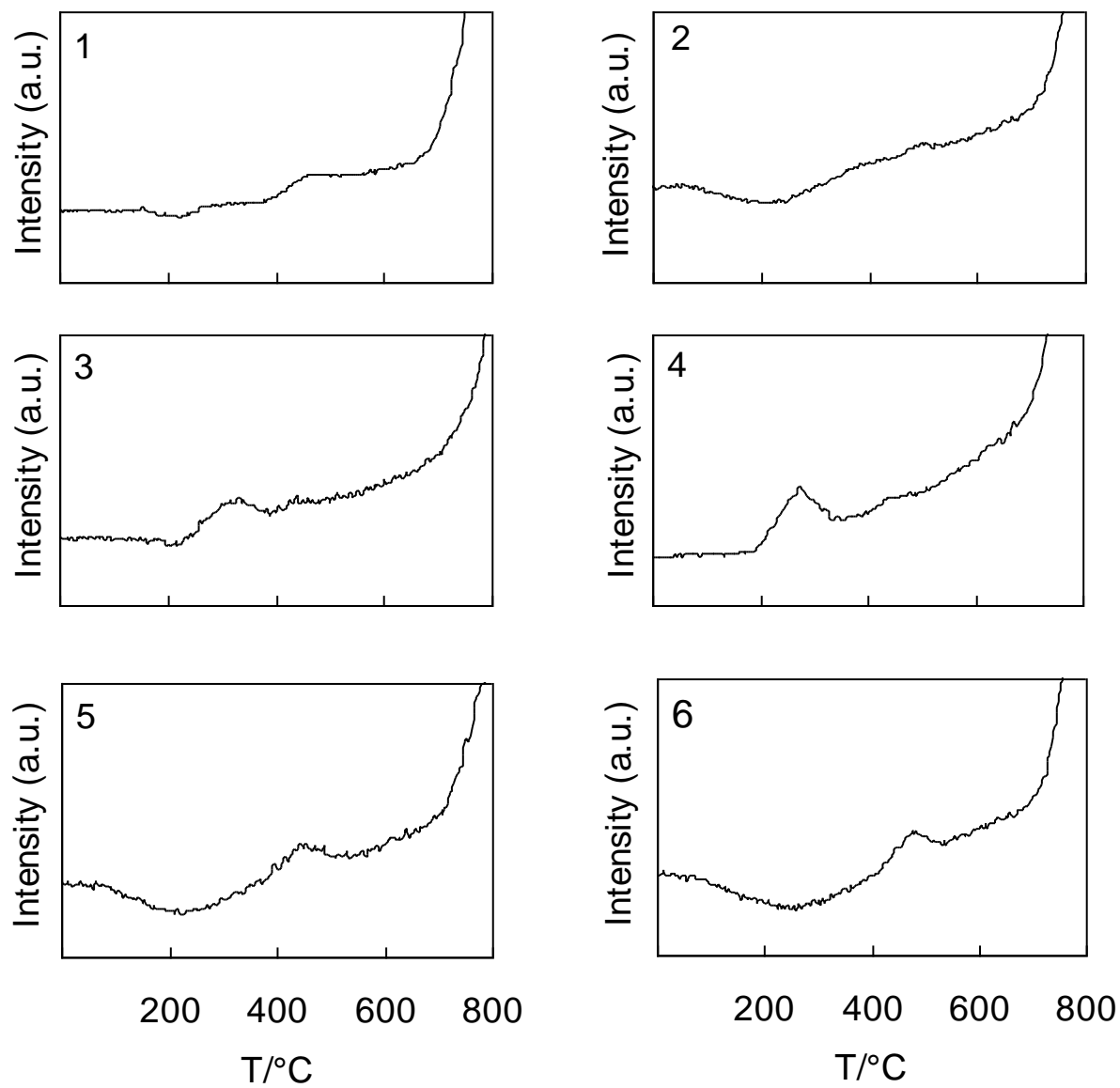
Fig. 5: TPR-MS spectrum of catalyst 3; m/z=15 signal relative to CH_4.

Fig. 6: EPR spectrum at 165 K of catalyst 1 (Table 1): (*a*) fresh, (*b*) after ten days ageing, (*c*) = (*a*) − (*b*). ($\ast$) $g = 2.35$; (o) $g \cong 2.02$.

Fig. 7: EPR spectrum at 135 K of catalyst 3 (*a*) and 6 (*b*) (Table 1), (*c*) = (*a*) − (*b*). (o): $g \cong 2.02$; (+): $g = 2.13$.

Fig. 8: Room temperature High-Frequency (240 GHz) EPR spectrum of (*a*) catalysts 3: (A) $g = 2.336$; (B) $g = 2.308$ and of (*b*) catalyst 6: (A) $g = 2.29$; (B) $g = 2.25$.

Fig. 9: *a*) CH_4 % conversion vs. temperature for the following samples: ($\blacktriangle$) catalyst 1, (O) catalyst 2, ($\blacklozenge$) catalyst 3, ($\bullet$) catalyst 4, ($\ast$) catalyst 5 and ($\blacksquare$) catalyst 6; *b*) comparison between samples: 3 ($\blacklozenge$), 7($\blacktriangle$) and 8 ($\blacksquare$).
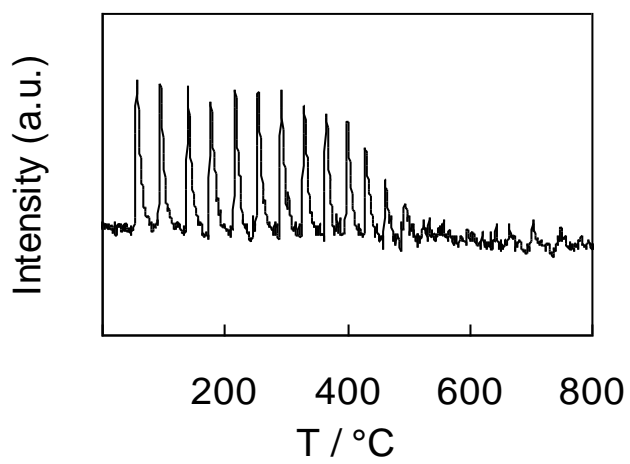
Fig. 3

21

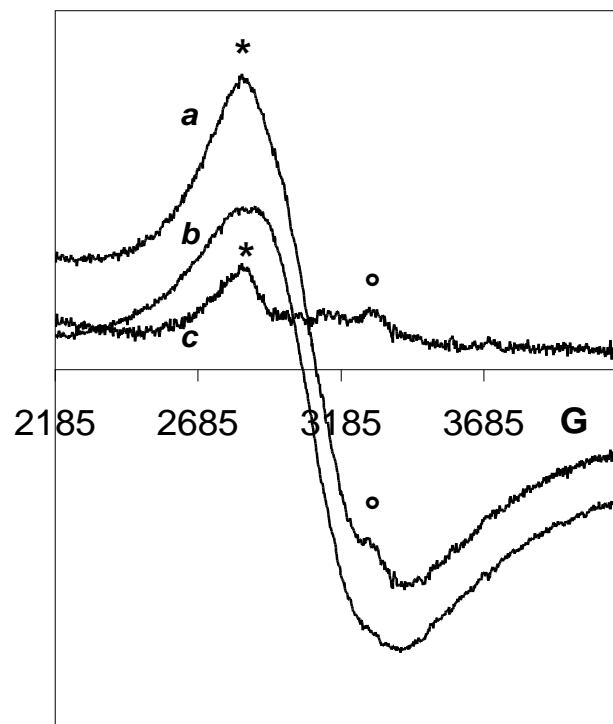**Fig. 4**

Fig. 5

2185   2685   3185   3685   G
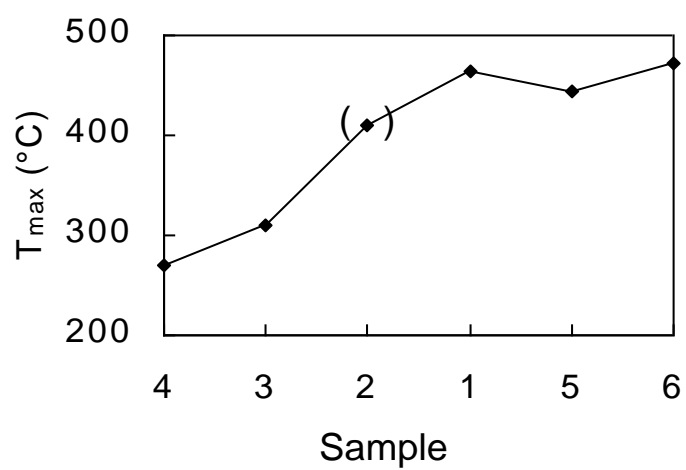
Manuscript no. MP-14/00

FIG. 6

FIG. 7

Manuscript no. MP-14/00

FIG. 8

FIG. 9

6

5

4

∇

∇

3

2

1

5　　　　　25　　　　　45　　　　　65

2θ

Fig. 1